

Interaction between hypersound and spin waves in antiferromagnetic MnCO_3

V. R. Gakel'

Institute of Physics Problems, USSR Academy of Sciences
(Submitted April 24, 1974)
Zh. Eksp. Teor. Fiz. 67, 1827–1842 (November 1974)

Coupled magnetoelastic waves in rhombohedral antiferromagnetic MnCO_3 , which possesses magnetic anisotropy of the easy plane type, are studied experimentally and theoretically. When the magnetic field is varied, the velocity and attenuation of the transverse hypersound undergo changes that have peculiar frequency and temperature dependences. These peculiarities are due to the interaction between the acoustic oscillations and nuclear spin waves. On the basis of a theoretical analysis of the multiply connected system consisting of spin (electron and nuclear) and acoustic oscillations, formulas are derived for the variation of the propagation velocity of the magnetoacoustic waves. These formulas describe satisfactorily the experimental data. The elastic and magnetoelastic constants and the nuclear spin parameters of the spin subsystem are obtained by comparing the theory with the experimental data.

1. INTRODUCTION

One of the most important characteristics of an antiferromagnet is the spectrum of the elementary excitations in it. The distinguishing feature of antiferromagnetic magnons is that their spectrum has a gap $f/\gamma = (H_a H_E)^{1/2}$, where H_a is the anisotropy field and H_E is the exchange field. Since $H_E \sim 10^5 - 10^6$ Oe and $H_a \sim 10^4$ Oe, it follows that the spin-wave spectrum falls in the millimeter and submillimeter bands, which are difficult to investigate experimentally. One of the few exceptions is the class of uniaxial antiferromagnets with anisotropy of the easy-plane type, in which the magnetization of the antiferromagnetic sublattices lies in a plane perpendicular to the axis. The spin-wave spectrum of these antiferromagnets has a gapless branch^[1,2]. The absence of a gap makes the spin-wave spectrum a sensitive instrument for the investigation of external and internal actions (of the magnetic field, of the deformations, of spontaneous striction, or of the hyperfine interaction) in such antiferromagnets^[1-6].

The magnetoelastic interaction leads to a mixing of the spin and acoustic waves. When the frequency and the wave vector of the acoustic and spin waves coincide, a resonant change should be observed in the damping and in the velocity of the sound and of the spin waves—the so-called magnetoacoustic resonance, which was theoretically investigated for easy-plane antiferromagnets by Bar'yakhtar et al.^[7]

In a preliminary communication^[8] we have presented the results of an investigation of the dependence of the speed of sound on the magnetic field in MnCO_3 , which is a rhombohedral easy-plane antiferromagnet (Neel temperature 32°K). In the antiferromagnetic state, we observed and investigated magnetoacoustic resonance in which the damping of the sound increased from 3–5 dB/cm far from resonance to more than 60 dB/cm in resonant fields, as well as a resonant change in the speed of sound V . A typical plot of the resonant variation of the speed of sound, obtained at 521.5 MHz and 1.65°K, is shown in Fig. 1. Measurements at different frequencies and temperatures have revealed a peculiar character of the magnetoacoustic resonance in MnCO_3 (see^[8]), namely, at frequencies below 640 MHz the value of the resonant field increases with increasing frequency and with decreasing temperature; above 640 MHz, the speed of sound decreases monotonically with decreasing mag-

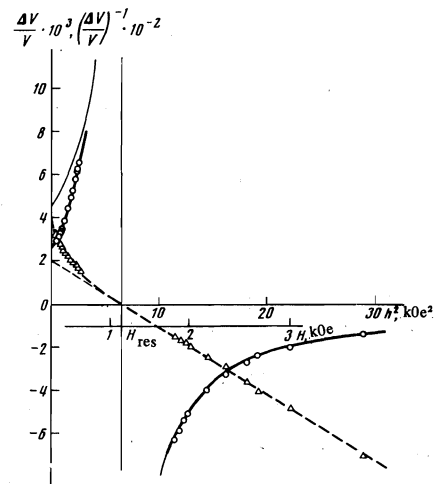


FIG. 1. Variation of the speed of sound, $\Delta V/V$, and of its reciprocal, $(\Delta V/V)^{-1}$, with changing magnetic field; $k \parallel X$, $V = 2.94 \times 10^5$ cm/sec, $H \parallel Y$, $f = 521.5$ MHz, $T = 1.65^\circ\text{K}$. Points—experimental values: \circ — $\Delta V/V$, \triangle — $(\Delta V/V)^{-1}$. Curves—theoretical plots: solid— $\Delta V/V$, dashed— $(\Delta V/V)^{-1}$; thick curves—in accordance with formula (26), thin curves—in accordance with (17); $h^2 = H(H + H_D)$.

netic field, and the change of the speed of sound is smaller the lower the frequency and the lower the temperature.

A theoretical analysis^[7] carried out without allowance for the influence of the nuclear spin subsystem does not account for the indicated singularities of the magnetoacoustic resonance in MnCO_3 . Our calculations of the multiply-connected system consisting of the electron and nuclear spin waves and acoustic oscillations in rhombohedral easy-plane antiferromagnets yielded the formula given in^[8], which describes well all the magnetoacoustic-resonance singularities investigated by us in MnCO_3 . We present below this theoretical calculation and the experimental data on the variation of the speed of sound as a function of the magnetic field for different types of acoustic oscillations, for different directions of the magnetic field, and for different temperatures and frequencies. A comparison of the experimental data and the theory have yielded for MnCO_3 the values of the magnetoelastic constants λ_3 and λ_4 , the values of the temperature-dependent and magnetoelastic gap in the spin-wave spectrum, and the frequency of the nuclear mag-

netic resonance. In addition, the elastic parameters of MnCO₃ were determined in the experiment.

2. THEORY

For uniaxial antiferromagnets, the magnetic energy per unit volume is given by^[9]

$$\begin{aligned} \mathcal{H}_m = & \frac{1}{2} B M^2 + \frac{1}{2} b M_z^2 + \frac{1}{2} a L_z^2 + q (L_x M_y - L_y M_x) \\ & - (M + \mathfrak{M}) H + A (\Lambda + M \mathfrak{M}) + (\mathfrak{M}^2 + \Lambda^2) / 2 \chi_n, \\ M = & M_1 + M_2, \quad L = M_1 - M_2, \quad \mathfrak{M} = \mathfrak{M}_1 + \mathfrak{M}_2, \\ \Lambda = & \mathfrak{M}_1 - \mathfrak{M}_2, \quad M \perp L, \quad \mathfrak{M} \perp \Lambda, \end{aligned} \quad (1)$$

where M_1 , M_2 , and \mathfrak{M}_1 , \mathfrak{M}_2 are respectively the electron and nuclear magnetizations of the sublattices per unit volume, B is the exchange constant, b and a are the anisotropy constants, q is the Dzyaloshinskii interaction constant, A is the hyperfine interaction constant, and χ_n is the nuclear susceptibility.

The magnetoelastic energy per unit volume takes in the case of rhombohedral antiferromagnets the form^[3,10]

$$\begin{aligned} \mathcal{H}_{me} = & \lambda_1 (u_{xx} + u_{yy}) L_x^2 + \lambda_2 u_{zz} L_z^2 + \lambda_3 [2u_{xy} L_x L_y \\ & + (u_{xx} - u_{yy}) (L_x^2 - L_y^2)] + \lambda_4 [2u_{xz} L_x L_z + u_{yz} (L_x^2 - L_y^2)] \\ & + \lambda_5 (u_{xx} + u_{yy}) (L_x^2 + L_y^2) + \lambda_6 u_{zz} (L_x^2 + L_y^2) \\ & + \lambda_7 [u_{xz} L_x L_z + u_{yz} L_y L_z] + \lambda_8 [u_{xy} L_x L_z + (u_{xx} - u_{yy}) L_y L_z], \\ u_{ik} = & \frac{\partial u_i}{\partial k} + \frac{\partial u_k}{\partial i} \quad (i, k = x, y, z; i \neq k), \quad u_{ii} = \frac{\partial u_i}{\partial i}, \end{aligned} \quad (2)$$

where Z is directed along the threefold axis of the crystal and X along the twofold axis. The influence of the piezomagnetic terms $p_{ikl} M_i L_j$ will be discussed below.

The elastic energy per unit volume in the case of rhombohedral crystals is^[11]

$$\begin{aligned} \mathcal{H}_{el} = & \frac{1}{2} c_{11} (u_{xx}^2 + u_{yy}^2) + \frac{1}{2} c_{33} u_{zz}^2 + c_{12} u_{xx} u_{yy} \\ & + c_{13} (u_{xx} + u_{yy}) u_{zz} + c_{14} (u_{xx} - u_{yy}) u_{yz} + \frac{1}{2} c_{44} (u_{yz}^2 + u_{xz}^2) \\ & + \frac{1}{2} (c_{11} - c_{12}) u_{xy}^2 + c_{14} u_{xy} u_{xz} - \sigma_{ij} u_{ij}, \end{aligned} \quad (3)$$

where σ_{ij} are the elastic stresses.

The total energy is equal to

$$\mathcal{H} = \mathcal{H}_m + \mathcal{H}_{el} + \mathcal{H}_{me}. \quad (4)$$

Minimizing the energy with respect to the different variables, we obtain the ground state for the case $H \perp Z$

$$\begin{aligned} \Lambda \parallel L, \quad \mathfrak{M} \parallel M, \\ M = \frac{1}{B} [H \sin(\varphi - \alpha) + H_D - A \mathfrak{M}], \quad M_z = 0 \\ \Lambda = -\chi_n A L, \quad \mathfrak{M} = \chi_n [H \sin(\varphi - \alpha) - A M], \quad u_{ij}^0 = u_{ij}^L + u_{ij}^S, \end{aligned} \quad (5)$$

$$\begin{aligned} \frac{L_z}{L} = & -\frac{S L^2}{a t} \sin 3\varphi - [\lambda_7 u_{yz}^0 + \lambda_8 u_{xy}^0] \cos \varphi - [\lambda_7 u_{yz}^0 + \lambda_8 (u_{xx}^0 - u_{yy}^0)] \sin \varphi, \\ M H \cos(\varphi - \alpha) = & -a_1 \sin 6\varphi - a_2 \cos 2\varphi + a_3 \sin 2\varphi. \end{aligned}$$

We use the following notation: $H_D = qL$ (4.4 kOe for MnCO₃) is the Dzyaloshinskii field, α is the angle between H and the X axis, φ is the angle between the projection of L on the basal plane and the X axis, u_{ij}^L is the spontaneous striction, which is determined by the magnetoelastic interaction, for example

$$\begin{aligned} u_{xy}^L = & t^{-1} [2(\lambda_3 c_{44} - \lambda_4 c_{14}) L_x L_y + (\lambda_3 c_{44} - \lambda_7 c_{14}) L_x L_z], \\ & t = c_{44}^2 - \frac{1}{2} (c_{11} - c_{12}) c_{44}, \\ S = & \lambda_7 \left(\lambda_4 \frac{c_{11} - c_{12}}{2} - \lambda_3 c_{14} \right) + \lambda_8 (\lambda_3 c_{44} - \lambda_4 c_{14}), \end{aligned} \quad (6)$$

u_{ij}^S is the strain in the stressed crystal, $aL/2 = H_a$ (3 kOe for MnCO₃) is the crystallographic anisotropy field,

$$a_1 = 3S^2 L^2 / 2at^2,$$

$$a_2 = -2(\lambda_3 u_{xy}^0 + \lambda_4 u_{xz}^0) L^2, \quad a_3 = -2[\lambda_3 (u_{xx}^0 - u_{yy}^0) + \lambda_4 u_{yz}^0] L^2. \quad (7)$$

Using the values $c_{ij} \sim 3 \times 10^{11}$ dyn/cm², $L \sim 10^3$ erg/G-cm³, $a = 2H_a/L \sim 10$, and $\lambda L^2 \sim 10^7$ erg/cm² (for hematite according to the data of^[12] and for MnCO₃ according to our data), we obtain from (5) and (6) $u_{ij}^L \sim 3 \times 10^{-5}$ and $L_z \sim 10^{-4} L$ (we shall henceforth neglect L_z).

In the antiferromagnetic state, the defects of the magnetic structure ΔL (for example, the crystal boundary) should lead, via the magnetoelastic interaction, to stresses σ and strains $u_{ij} \sim u_{ij}^L \sim 3 \times 10^{-5}$. Substitution of these values in (7) yields for MnCO₃:

$$|a_1| \ll |a_2| \sim |a_3|, \quad |A_{2,3}| \sim 0.4 \text{ kOe}^2, \quad (8)$$

where $A_{2,3} = 2Ba_{2,3}$. (For MnCO₃, the exchange field $H_E = BL = 320$ kOe, and thus $B \sim 300$.)

From (5), neglecting the term $a_1 \sin 6\varphi$, we get

$$[H \sin(\varphi - \alpha) + H_D] H \cos(\varphi - \alpha) = -\frac{1}{2} A_2 \cos 2\varphi + \frac{1}{2} A_3 \sin 2\varphi. \quad (9)$$

From this, at $\alpha = -\pi/2$ ($H \parallel Y$) and at small φ we obtain approximately $h^2 \sin 2\varphi = A_2 \cos 2\varphi - A_3 \sin 2\varphi$, whence

$$\text{tg } 2\varphi = A_2 (h^2 + A_3)^{-1}, \quad (10)$$

$$h^2 = H(H + H_D). \quad (10a)$$

It follows from (10) that at $H = \infty$ we have $\varphi = 0$, i.e., $L \perp H$ and $M \parallel H$; with decreasing H , the angle φ increases, i.e., M and H become nonparallel. A similar behavior of the vector M (and consequently L) is obtained also at $H \parallel X$.

Oscillations of the spins (electron and nuclear) and of the deformations about the equilibrium values obtained above are described by the equations^[13,14]

$$\begin{aligned} \frac{1}{\gamma_0} \dot{l} = & [L \times \frac{\partial \mathcal{H}}{\partial M}] + [M \times \frac{\partial \mathcal{H}}{\partial L}], \quad \frac{1}{\gamma_0} \dot{m} = [L \times \frac{\partial \mathcal{H}}{\partial L}] + [M \times \frac{\partial \mathcal{H}}{\partial M}], \\ \frac{1}{\gamma_n} \dot{\lambda} = & [\Lambda \times \frac{\partial \mathcal{H}}{\partial \mathfrak{M}}] + [\mathfrak{M} \times \frac{\partial \mathcal{H}}{\partial \Lambda}], \quad \frac{1}{\gamma_n} \dot{\mu} = [\Lambda \times \frac{\partial \mathcal{H}}{\partial \Lambda}] + [\mathfrak{M} \times \frac{\partial \mathcal{H}}{\partial \mathfrak{M}}], \\ \rho \ddot{u}_i = & \frac{\partial^2 \mathcal{H}}{\partial x \partial u_{ix}} + \frac{\partial^2 \mathcal{H}}{\partial y \partial u_{iy}} + \frac{\partial^2 \mathcal{H}}{\partial z \partial u_{iz}} \quad (i = x, y, z), \end{aligned} \quad (11)$$

where l , m , λ , μ , and u_{ijk} (the aggregate of which will be designated $\{x\}$) are small deviations of the quantities L , M , Λ , \mathfrak{M} , and u_{ijk} (aggregate $\{X\}$) from the equilibrium values $\{X_0\}$.

We have a solution of the system (11) in the form

$$x = x_0 \exp[-i(\omega t - \mathbf{k}r)]. \quad (12)$$

Substituting (12) in (11) and using the obtained equilibrium values $\{X_0\}$, we get a system of 15 homogeneous equations. From the condition that a nontrivial solution exists (the determinant of the system is equal to zero), we obtain the dispersion equation. At $L \perp H$, i.e., in the case of strong fields, and for a wave vector $\mathbf{k} \parallel X$ and $H \parallel Y$, the dispersion equation takes the form ($f = \omega/2\pi$)

$$\begin{aligned} & (-f^2 + f_{1e}^2) (-f^2 + f_{1nuc}^2) (-f^2 + f_{2e}^2) (-f^2 + f_{2nuc}^2) \rho^2 (V^2 - V_2^2) (V^2 - V_3^2) \\ & + P_{44,33} (-f^2 + f_{2e}^2) (-f^2 + f_{2nuc}^2) (-f^2 + f_{nuc}^2) \gamma_e^2 \\ & + P_{77,88} (-f^2 + f_{1e}^2) (-f^2 + f_{1nuc}^2) (-f^2 + f_{nuc}^2) \gamma_e^2 \\ & + [4H_E^2 L^2 (\lambda_4 \lambda_8 - \lambda_3 \lambda_7) + P_{47,38} H_{\Delta 2}^2] (-f^2 + f_{nuc}^2)^2 \gamma_e^4 = 0. \end{aligned} \quad (13)$$

Here V_2 and V_3 are the velocities of the transverse sound, obtained from the equation

$$\left(V_{2,3}^2 - \frac{c_{11}-c_{12}}{2\rho} \right) \left(V_{2,3}^2 - \frac{c_{44}}{\rho} \right) = \frac{c_{44}^2}{\rho^2}; \quad (14)$$

f_{1e} , f_{1nuc} and f_{2e} , f_{3nuc} are respectively the lower and upper electron-like and nuclear-like branches of the spin-wave spectrum, defined by the equations

$$[-f^2 + (f_{ie})^2](-f^2 + f_{nuc0}^2) = \gamma_e^2 H_\Delta^2 f^2 \quad (i=1, 2),$$

where

$$\begin{aligned} (f_{1e})^2/\gamma_e^2 &= h^2 + H_{\Delta 1}^2 + \beta H_E^2 (dk)^2, \\ (f_{2e})^2/\gamma_e^2 &= 2H_e H_B + H_D (H + H_D) + \beta H_E^2 (dk)^2 \end{aligned} \quad (14a)$$

($f_{2e}^0 \approx 124$ GHz for MnCO_3 [15]). It follows from (14a) that

$$(-f^2 + f_{ie}^2)(-f^2 + f_{nuc0}^2) = [-f^2 + (f_{ie}^0)^2](-f^2 + f_{nuc0}^2) + \gamma_e^2 H_\Delta^2 f^2 \quad (i=1, 2); \quad (14b)$$

$H_\Delta^2 = -H_E \Lambda \Lambda = A^2 \chi_n L H_E = bT^{-1}$ is the gap of the spin-wave spectrum and is due to the influence of the nuclear spins on the electron spins via the hyperfine interaction [4]; $H_{\Delta 1}^2 = -4H_E L [\lambda_4 u_{yz}^0 + \lambda_3 (u_{xx}^0 - u_{yy}^0)]$ is the gap of the spin-wave spectrum, due to the magnetoelastic interaction; $f_{nuc0} = \gamma_{nuc} \Lambda L$ (640 MHz for MnCO_3) is the frequency of the nuclear magnetic resonance in the effective field of the electron sublattices that act on the nuclei via the hyperfine interaction;

$$\begin{aligned} P_{ij,kl} &= 4H_E L^3 \left[\lambda_i \lambda_j \left(\rho V^2 - \frac{c_{11}-c_{12}}{2} \right) + (\lambda_j \lambda_k + \lambda_i \lambda_l) c_{44} + \lambda_k \lambda_l (\rho V^2 - c_{44}) \right], \\ H_{\Delta 2}^2 &= -4H_E L [\lambda_7 u_{xz}^0 + \lambda_8 (u_{xx}^0 - u_{yy}^0)]. \end{aligned}$$

The term $\beta H_E^2 (dk)^2$ appears when allowance is made in the Hamiltonian (1) for the exchange energy $\alpha (\partial L_i / \partial x_k)^2$ [16], $\alpha = \beta B d^2$, d is the lattice constant, and $\beta \sim 1$.

It follows from (13) that magnetoacoustic resonance will be observed when the acoustic-oscillation spectra intersect each electron-like and nuclear-like branch of the spin-wave branch, i.e., a resonant change in the velocities V_2 and V_3 of the transverse sound and in the velocity of the spin waves will occur when the frequencies of the acoustic oscillations coincide with the frequency of the spin waves $f_{1e}(H)$, f_{2e} , $f_{1nuc}(H)$, and f_{2nuc} . (The wave vectors \mathbf{k} are identically equal, since we are seeking a solution in the form of (12) with identical \mathbf{k} for all the oscillation modes.)

At $|(f - f_{2nuc})/f_{2nuc}| > 0.3$ and $|f - f_{2nuc}| > 1$ MHz ($f_{2nuc} \approx 635$ MHz for MnCO_3), the influence of the upper electron branch and the nuclear branch of the spin waves is negligibly small, and Eq. (13), with allowance for (14b), takes the form

$$[-f^2/\gamma_e^2 + h^2 - G] \rho^2 (V^2 - V_2^2) (V^2 - V_3^2) + P_{44,33} = 0, \quad (15)$$

$$G = \frac{f^2}{f_{nuc0}^2 - f^2} H_\Delta^2 - H_{\Delta 1}^2 - \beta H_E^2 (dk)^2. \quad (16)$$

For the change in the sound velocity, using (14), we obtain the formula given in [8]:

$$\Delta V_{2,3}/V_{2,3} = -K_{V_{2,3}} [-f^2/\gamma_e^2 + h^2 - G]^{-1},$$

where

$$\begin{aligned} K_{V_{1,2}} &= \frac{P_{44,33}}{2\rho^2 V_{2,3}^2 (V_{2,3}^2 - V_{3,2}^2)} \\ &= \frac{2H_E L^3 \lambda_4^2 \gamma^2}{\rho V_{2,3}^2 (V_{2,3}^2 - V_{3,2}^2)} \left\{ 1 + \frac{\lambda_3}{\lambda_4} \frac{1}{\gamma^2} \left[\gamma^2 \left(V_{2,3}^2 - \frac{c_{44}}{\rho} \right) \right]^{1/2} \right\}^2, \end{aligned} \quad (17)$$

$$\gamma^2 = V_{2,3}^2 - (c_{11} - c_{12})/2\rho.$$

Exactly the same expression is obtained also at $\mathbf{H} \parallel \mathbf{X}$.

The first term in G [Eq. (16)] is a result of the influence of the nuclear spin subsystem on the magnetoelastic waves, and determines the singularities of the magnetoacoustic resonance in antiferromagnets with easy-plane anisotropy, namely, the temperature and frequency dependence indicated in the introduction. These singularities come into play most strongly at $f \approx f_{nuc0}$, both as $G \rightarrow \pm \infty$ and as $f - f_{nuc0} \rightarrow \pm 0$. In the frequency region of interest to us ($f \sim f_{nuc0}$), we shall henceforth neglect the terms $\beta H_E^2 (dk)^2$ and f^2/γ_e^2 in (16) and (17). Indeed, for MnCO_3 at $f \leq 1$ GHz we have $\beta H_E^2 (dk)^2 \approx f^2/\gamma_e^2 \leq 0.1$ kOe², which is less than the uncertainty of h^2 connected with the finite width of the spin-wave spectrum.

In the case of different directions of the wave vector \mathbf{k} , and at arbitrary angle φ , the dispersion equation takes the form

$$\begin{aligned} \frac{\rho}{4H_E L^3} \left[-\frac{f^2}{\gamma_e^2} + h^2 - G \right] (V^2 - V_{10}^2) (V^2 - V_2^2) (V^2 - V_3^2) \\ + b_1^2 (V^2 - V_2^2) (V^2 - V_3^2) + b_2^2 (V^2 - V_{10}^2) (V^2 - V_{30}^2) \\ + b_3^2 (V^2 - V_{10}^2) (V^2 - V_{20}^2) + 2b_2 b_3 (V^2 - V_{10}^2) c/\rho = 0, \end{aligned} \quad (18)$$

where V_{10} , V_2 , and V_3 are the propagation velocities of the three types of acoustic oscillations that exist at the given direction \mathbf{k} . The sound velocities V_2 and V_3 are determined from the equation

$$(V_{2,3}^2 - V_{20}^2) (V_{2,3}^2 - V_{30}^2) = c_{11} c^2 / \rho^2, \quad (19)$$

and the direction of the polarization vector \mathbf{R} is determined from the equation

$$\text{tg } \beta_{2,3} = \frac{c}{\rho} \frac{1}{V_{2,3}^2 - V_{20}^2}. \quad (20)$$

The values of the parameters obtained in (18)–(20) for the cases k_x , k_y , and k_z are given in Table I.

For a wave vector $\mathbf{k} \parallel \mathbf{X}$ we have longitudinal sound (V_{10} , \mathbf{R}_x), transverse "fast" sound (V_2 , \mathbf{R}_2), and transverse "slow" sound (V_3 , \mathbf{R}_3), with $V_3 < V_2$; at $\mathbf{k} \parallel \mathbf{Y}$ we have transverse sound (V_{10} , \mathbf{R}_x), quasilongitudinal sound (V_2 , $\mathbf{R}_2 \approx \mathbf{R}_y$), and quasitransverse sound (V_3 , $\mathbf{R}_3 \approx \mathbf{R}_x$); at $\mathbf{k} \parallel \mathbf{Z}$ we have two transverse sounds with equal velocities ($V_{10} = V_2 = (c_{44}/\rho)^{1/2}$) and with polarizations that are arbitrary in the XY plane (but are mutually perpendicular), as well as longitudinal sound ($V_3 = (c_{33}/\rho)^{1/2}$, \mathbf{R}_z).

Inclusion of the piezomagnetic terms $p u_k L_i M_j L_j$ in the Hamiltonian (4) leads to a nonzero equilibrium $M_z \sim p \cos 3\varphi$ and to an additional contribution to u_{ik}^0 . In addition, at $\mathbf{H} \parallel \mathbf{Y}$, the piezomagnetic terms ensure interaction with the lower electron-nuclear branch in accordance with formula (7), with coefficients $K_{V_{pm}}$ of the longitudinal sound at $\mathbf{k} \parallel \mathbf{X}$, of the quasilongitudinal and quasitransverse sound at $\mathbf{k} \parallel \mathbf{Y}$, of the transverse sound with polarization u_i at $\mathbf{k} \parallel \mathbf{Z}$, and also interaction with the upper electron-nuclear branch of the longitudinal sound at $\mathbf{k} \parallel \mathbf{Z}$. The coefficients $K_{V_{pm}}$ are connected with the previously discussed coefficients $K_{V_{me}} = \{K_{V_j}\}$ by the relation $K_{V_{pm}} = (p/\lambda)^2 (H_\Delta^2 / H_E^2) K_{V_{me}}$. For MnCO_3 we have $H_\Delta^2 / H_E^2 \approx 6 \times 10^{-5} / T$ (where T is in $^\circ\text{K}$).

TABLE I.

Direction of \mathbf{k}	Parameter						
	b_1	b_2	b_3	c	cV_{30}^2	cV_{20}^2	cV_{10}^2
$\parallel \mathbf{X}$	$-\lambda_3 \sin 2\varphi$	$\lambda_3 \cos 2\varphi$	$-\lambda_4 \cos 2\varphi$	c_{14}	c_{44}	$(c_{11} - c_{12})/2$	c_{11}
$\parallel \mathbf{Y}$	$\lambda_3 \sin 2\varphi$	$\lambda_3 \sin 2\varphi$	$-\lambda_4 \sin 2\varphi$	$-c_{14}$	c_{44}	c_{11}	$(c_{11} - c_{12})/2$
$\parallel \mathbf{Z}$	$\lambda_4 \cos 2\varphi$	$-\lambda_4 \sin 2\varphi$	0	0	c_{33}	c_{44}	c_{44}

3. EXPERIMENT. PROCEDURE

We used MnCO_3 samples grown by the hydrothermal method¹⁾ in the form of rectangular parallelepipeds with dimensions 2–3.5 mm. A pulse and phase-pulse procedure was used for the acoustic measurement (Fig. 2a). A continuous hf signal (frequency $f = 200\text{--}800$ MHz from a G3-20 generator) was branched into two channels. In the first channel, the pulse-modulated signal passed through a calibrated coaxial line of variable length L , limited by attenuators 3 (5 dB) to improve the traveling-wave regime in the line, and then, transformed to sound, passed through sample 1, was again transformed into an hf signal, and was fed to the mixer 5. Almost complete prevention of leakage of the hf signal, bypassing of the conversion into sound, was prevented by silver-coating the acoustic converters 2.

In the second channel, the continuous hf signal passed through a variable attenuator 4, covered a path L_2 , entered the mixer 5, where it was mixed with the signal of the first channel and the signal of the G3-20 heterodyne. The difference-frequency signal (8–10 MHz), after passing through a broad band amplifier USH-10, was fed to an S1-15 oscilloscope.

If the second channel is blocked, i.e., $U_2 = 0$, we obtain a pulsed procedure for measuring the absolute value of the speed of sound. From the acoustic echo pulses observed on the oscilloscope (Fig. 2b, $U_2 = 0$), using the time-interval meter I2-16/17, we determine the speed of the sound. The error in the measurement of the absolute value of the speed of sound is 1.5–2%.

At $U_2 \neq 0$ we obtain a phase-pulse procedure with which to measure, by comparing the phases of the signals in the first and second channels, the relative change $\Delta V/V$ of the speed of sound, with accuracy 10^{-4} .

We have observed on the oscilloscope screen mutual cancellation of the signals of the first and second channels (Fig. 2b):

$$U_1 = U_2, \quad \varphi_1 = \varphi_2 + (2n+1)\pi.$$

The phase shift φ_1 is represented in the form $\varphi_1 = \varphi_L + \varphi_V$, where $\varphi_L = 2\pi fL/c$ is the phase shift in the variable-length line, $\varphi_V = 2\pi fl/V$ is the phase shift in the sample, and $\varphi_2 = 2\pi fL_2/c$ is the phase advance in the shift channel. Thus,

$$\frac{fL}{c} + \frac{fl}{V} = \frac{fL_2}{c} + \left(n + \frac{1}{2}\right),$$

where c is the speed of light and V is the speed of sound. The change of the phase shift φ_V with changing speed of sound was offset by a change in the phase shift φ_L by varying the length of the line, so that $\varphi_1 = \varphi_L + \varphi_V = \text{const}$. Then

$$\frac{\Delta V}{V} = \frac{V}{c} \frac{\Delta L}{l} \quad (\text{at } f = \text{const}), \quad (21)$$

where l is the path length of the sound pulse in the sample, and ΔL is the change of the length of the measuring line. Owing to the strong damping of the sound near the resonance, the measurements were performed as a rule with the first sound pulse (in this case l was the length of the sample).

In view of the small dimensions of the samples (2–3.5 mm), it was necessary to work with short pulses. The matching of all the circuits and the large bandwidth of the USH-10 amplifier (16 MHz) made it possible to work with 0.2–0.3 μsec pulses. The acoustic converters were X-cut LiNbO_3 plates (odd harmonics of acoustic

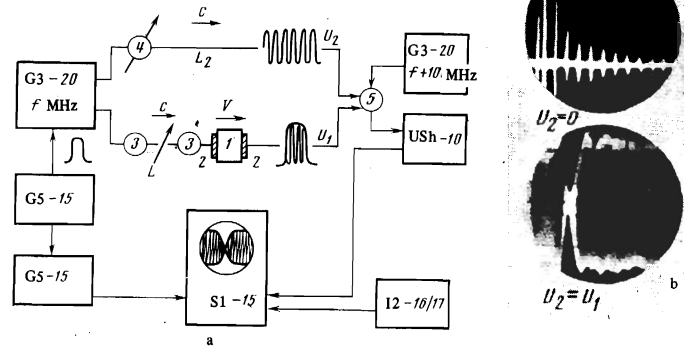


FIG. 2. a) Block diagram of measuring installations: pulsed ($U_2 = 0$) and phase-pulsed ($U_2 = U_1, \varphi_1 + \varphi_2 + (2n+1)\pi$); b) the corresponding oscillograms.

resonance of the plates were excited, the first harmonic being ~ 80 MHz).

The orientation of the plane of polarization of the transverse sound of the acoustic converters relative to the crystallographic directions of the sample was determined accurate to 4% by alignment with the direction of the X and Z axes of potassium biphthalate (PBP), which are the directions of the polarization of the normal acoustic oscillations of the Y-cut PBP (PBP was chosen because of the low values of the sound velocities in it²⁾).

For the acoustic contact we used a thin layer of GKZh silicone oil with low solidification temperature. To produce the magnetic field, we used an electromagnet of the S. P. Kapitza system and a superconducting solenoid. The magnetic field was in the basal plane of the sample (XY plane) along the X or Y axes with accuracy $2\text{--}3^\circ$. The value of the magnetic field was measured with the aid of an IMI-3 instrument (for the electromagnet) with accuracy 0.5% and by determining the current (for the solenoid) with relative accuracy 0.5% and absolute accuracy $2\text{--}3\%$ as calibrated against a milliweber meter.

There were four sources of errors in the measurement of $\Delta V/V$.

1. Since the pulse waveform differs from rectangular, the compensation of the signal occurs in a narrow region of the pulse. When this region is fixed relative to the oscilloscope sweep, the obtained accuracy in the measurement of $\Delta V/V$ is 0.5×10^{-4} (the error in the measurement of L is smaller by several times). At larger speeds of sound or smaller dimensions of the crystals, this error increases by 1.5–2 times.

2. A small deviation of the wave in the measurement line L from the traveling-wave regime led to a dependence of the measurement of $\Delta V/V$ on the line length (less than 0.4×10^{-4} at $\Delta L = \lambda/4$).

3. The appreciable difference between the delay times in the first and second channels (τ_1 and τ_2) led to a dependence of the measurements of $\Delta V/V$ on the frequency:

$$\frac{\Delta V}{V} = \frac{V}{c} \frac{\Delta L}{l} + \frac{V}{fl} \Delta f(\tau_1 - \tau_2) \approx \frac{V}{c} \frac{\Delta L}{l} + \frac{\Delta f}{f}$$

($\tau_1 \approx l/V \gg \tau_2 = L_2/c$). Owing to the drift of the generator frequency, this led to a smooth change of $\Delta V/V$ and amounted, after two or three hours of heating of the generator, to $(0.7 \pm 0.7) \times 10^{-4}$ at an experiment duration 3–40 min (and accordingly $(0.07 \pm 0.07) \times 10^{-4}$ between

neighboring experimental points, something that was taken into account in the reduction of the results.

4. In the region of the resonance, when the attenuation of the sound is strongly increased in the sample, it was necessary to vary the amplitude U_2 (by means of attenuator 3), and this led to a slight change in the generator frequency and accordingly to a measurement error $\Delta V/V \leq 0,5 \times 10^{-4}$.

In the case of weak coupling between the acoustic and spin waves (i.e., small values of $|\Delta V/V|_{\max}$), which takes place for the (V_{10}, k_y) acoustic mode and at $G < -20$ for all the acoustic modes, the damping of the sound changes little in the entire range of fields, so that the error of Item 4 was eliminated, the error of Item 2 decreased (since $\Delta L \ll \lambda/4$ in this case), and in addition, this has made it possible to carry out the measurements with the aid of the second echo pulse ($l = 3d$), thus decreasing by several times the error of Item 1. The resultant error in the measurement of $\Delta V/V$ (obtained by adding the variances of the independent errors) ranged for our samples at low velocities from 10^{-4} at $|\Delta V/V|_{\max} \approx 60 \times 10^{-4}$ to 0.4×10^{-4} at $|\Delta V/V|_{\max} \approx 10 \times 10^{-4}$, and was larger by 1.5 times at higher velocities.

4. RESULTS. ELASTIC PARAMETERS

The measurements yielded the following values of the propagation velocities V and the direction of polarization vector³⁾ \mathbf{R} of the transverse acoustic oscillations in MnCO_3 (V is in units of 10^5 cm/sec, and the angle β is measured from the Z axis):

a) wave vector $\mathbf{k} \parallel \mathbf{X}$

$$V_2 = 4,55 \pm 0,06, \beta_2 = 51^\circ \pm 4^\circ; \quad V_3 = 2,94 \pm 0,05, \beta_3 = 39^\circ \pm 4^\circ; \quad (22a)$$

b) $\mathbf{k} \parallel \mathbf{Y}$

$$V_{10} = 4,14 \pm 0,08, \mathbf{R}_{10} \parallel \mathbf{X}; \quad V_3 = 3,39 \pm 0,08, \mathbf{R}_3 \parallel \mathbf{Z}; \quad (22b)$$

c) $\mathbf{k} \parallel \mathbf{Z}$

$$V_{10} = 3,41 \pm 0,07, \mathbf{R}_{10} \parallel \mathbf{X}; \quad V_2 = 3,41 \pm 0,07, \mathbf{R}_2 \parallel \mathbf{Y}. \quad (22c)$$

The values of the sound velocities in the temperature interval $80-1.5^\circ$ remained constant within the limits of the measurement error. The obtained velocities and polarizations of the sound agree with Eqs. (19) and (20) within the limits of the measurement errors and yield $|c_{14}/\rho| = (5.3 \pm 1.2) \times 10^{10}$ cm² sec⁻². Using the obtained value of $|c_{14}/\rho|$ and $V_{10}|_{\mathbf{k}=\mathbf{k}_X} = (c_{11}/\rho)^{1/2} = 7.4 \times 10^5$ cm/sec (taken from the data for calcite^[17], in which the velocity of sound is close to ours), we obtain from (19) at $\mathbf{k} \parallel \mathbf{Y}$ the value $V_3 = (3.31 \pm 0.10) \times 10^5$ cm/sec, which agrees with the measured value within the limits of errors.

For the five types of the acoustic oscillations (V_2 and V_3 at k_x ; V_{10}, V_3 at k_y ; V_{10} at k_z) we measured the dependence of the sound velocity on the magnetic field for eleven values of the frequency in the range 200–800 MHz at different orientations of the magnetic field in the basal plane and at temperatures from 4.2 to 1.65°K. The obtained data were reduced with a computer by least squares using formula (17)⁴⁾. The reduction has shown that the experimental data agree well with the theoretical relation (17) at $H \geq 2$ kOe for sample I and at $H \geq 3$ kOe for sample II. At $1 \text{ kOe} \leq H \leq 2-3$ kOe, the parameters G (at fixed K_V) or K_V (at fixed G), obtained from the data reduction, decrease with decreasing field H , and at $H \leq 1$ kOe the deviation of the experimental values of

$\Delta V/V$ in formula (17) exceed the measurement error. All this indicates that formula (17) is not valid in weak fields. The reason for the deviation from the theory is the fact that the condition $\mathbf{L} \perp \mathbf{H}$ (at which formula (17) was obtained) in weak fields ceases to be satisfied and the direction of \mathbf{L} begins to depend on the value of the magnetic field (see (10)), and this causes an additional change in the speed of sound by virtue of the anisotropy of the magnetoelastic interaction (2).

5. ANISOTROPY OF THE MAGNETOELASTIC INTERACTION

The anisotropy of the magnetoelastic interaction leads to a dependence of the sound velocity on the direction of the vector \mathbf{L} in the basal plane (i.e., on φ). From (18) and Table I, in the case of an arbitrary angle φ , we obtain Eq. (17) with a coefficient $K_V(\varphi)$ that depends on φ . For the acoustic modes (see the last paragraph of Sec. 2) we have the following:

1) In the longitudinal (V_{10}, R_x, k_x), (V_3, R_z, k_z), quasilongitudinal (V_2, R_2, k_y), transverse ($V_2 R_y, k_z$) and quasitransverse (V_3, R_3, k_y) modes we have

$$K_V(\varphi) = K_{V \max} \sin^2 2\varphi; \quad (23)$$

2) for the transverse acoustic modes (V_{10}, R_x, k_y), (V_{10}, R_x, k_z), (V_2, β_2, k_x), (V_3, β_3, k_x) we obtain

$$K_V(\varphi) = K_{V \max} \cos^2 2\varphi. \quad (24)$$

We measured the dependence of the sound velocity on φ for the (V_{10}, R_x, k_z) mode at $T = 4.2^\circ \text{K}$, $f = 544$ MHz, and $H = 5.70$ kOe (Fig. 3) with \mathbf{H} rotated in the basal plane (the magnetic field was strong enough to satisfy the condition $\mathbf{L} \perp \mathbf{H}$). As seen from Fig. 3, the result agrees well with formula (24) (the curve in the figure is proportional to $\cos^2 2(\varphi - 3^\circ)$). The angle 3° is the sum of the deviation of \mathbf{L} from perpendicularity to \mathbf{H} (1° at $H = 5.70$ kOe; see (10) and (28a)), and the error of 2° in the orientation of $\mathbf{L} \parallel \mathbf{X}$.

In view of the dependence of the direction of the vector \mathbf{L} on the magnetic field (formula (10)), it is necessary in weak fields to use the generalized formula (18), even when \mathbf{H} is oriented along the X or Y axis. Substituting the expression for the dependence of the angle φ on the field (see (10)) in (23) and (24), we obtain in these cases a generalization of formula (17) to include the entire range of fields (including weak fields): for the acoustic modes 1)

$$\frac{\Delta V}{V} = - \frac{K_V(45^\circ)}{h^2 - G} \frac{A_2^2}{(h^2 + A_3)^2 + A_2^2} \quad (25)$$

and for modes 2)

$$\frac{\Delta V}{V} = - \frac{K_V(0)}{h^2 - G} \left[1 - \frac{A_2^2}{(h^2 + A_3)^2 + A_2^2} \right]. \quad (26)$$

Here G is defined in (16), h^2 is defined in (10a), and A_2 and A_3 depend on the sample, since they are determined by the imperfections of the crystal (see (7) and (8)).

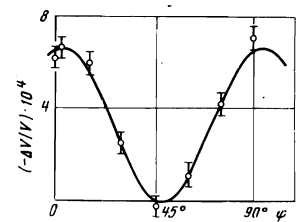


FIG. 3. Dependence of the speed of sound on the angle φ between the direction of the antiferromagnetic vector \mathbf{L} and the twofold axis X .

From (17) and (24) it follows that

$$\varphi = \frac{1}{2} \arctg F, \quad (27)$$

where

$$F^2 = \left(\frac{\Delta V}{V}\right)_0 / \frac{\Delta V}{V} - 1, \quad \left(\frac{\Delta V}{V}\right)_0 = -\frac{K_V(0)}{h^2 - G}. \quad (27a)$$

From (10) and (27) we get

$$F^{-1} = (h^2 + A_3) / A_3, \quad (27b)$$

which is a different version of formula (26).

The experimental data agree well with formula (27b) at $H \geq 300$ Oe (Fig. 4) and yield for sample I

$$A_3 = 1.2 \pm 0.6 \text{ kOe}^2, \quad A_2 = 1.8 \pm 0.4 \text{ kOe}^2 \quad (28a)$$

and for sample II

$$A_3 = 0.7 \pm 0.3 \text{ kOe}^2, \quad A_2 = 2.8 \pm 0.2 \text{ kOe}^2. \quad (28b)$$

The large range of fields used in the experiment (h^2 ranges from 0 to 150 kOe^2), and the accuracy of our measurements of $\Delta V/V$, have made it possible to determine uniquely all the parameters in (26). The obtained values of A_2 and A_3 agree in order of magnitude with the estimate of these values in (8).

The deviations from the theory that are opposite to those in the preceding case (increase of $|\Delta V/V|$ in weak fields) were observed in the measurement of the sound velocity in the case of the (V_3, k_y) mode at $H \parallel Y$ ($T = 4.2^\circ \text{K}$, $f = 260$ MHz, sample II)—see Fig. 5. In this case formula (23) at $L \perp H$ calls for $\Delta V/V = 0$, as was indeed observed at $H \geq 3$ kOe. At $H \leq 3$ kOe the ratio $\Delta V/V$ begins to increase with decreasing field. The theoretical dependence in accordance with formula (25) with values of A_2 and A_3 taken from (28b) (at $G = 0$ and

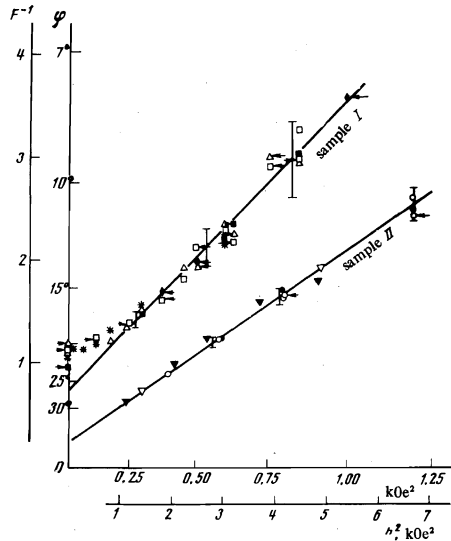


FIG. 4. Dependence of the quantity F^{-1} (see (27a)) and of the value of the angle φ between M and H , calculated from this dependence by means of formula (27), on the magnetic field (h^2 , see (10a)) for samples I and II. The theoretical straight lines are plots of (27b). The experimental points correspond to the following:

k	H	V · 10 ⁻³	f = 250		660		668		682		780	
			T = 4.2	1.65	4.2	4.2	4.2	1.65	1.65			
X	X	2.94	○	●	△	*	□	■	◆			
X	Y	2.94	○	●	△	*	□	■	◆			
X	Y	4.55	○	●	△	*	□	■	◆			
Y	Y	4.14	▽	▼	→△		□	■	◆			

Here V is in cm/sec, f in MHz, and T in K.

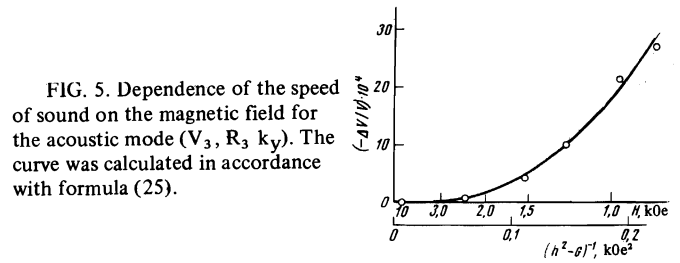


FIG. 5. Dependence of the speed of sound on the magnetic field for the acoustic mode ($V_3, R_3 k_y$). The curve was calculated in accordance with formula (25).

6. MAGNETOELASTIC PARAMETERS

The coefficient $K_V(0)$ in formula (26) is determined by the reduction of the experimental data for the case $G > -13 \text{ kOe}^2$, when $|\Delta V/V|_{\max}$ assumes large values. The individual error in the determination of K_V was 5–15%. The data reduction has shown that the coefficient K_V does not depend on the temperature or the frequency, is the same for H_x and H_y , but depends on the mode of the acoustic oscillations. The values of K_V , which are weighted averages of the values obtained for a given acoustic mode of the values for different acoustic modes and magnetic field directions, are given in Table II in units of 10^{-4} kOe^2 . From formula (18) and from Table I, by using the measured sound velocities (22) and the values of K_{V_2} and K_{V_3} at $k \parallel X$ (Table II), we obtain

$$k \parallel Z: K_{V_0} = 543 \cdot 10^{-4} \text{ kOe}^2, \quad (29)$$

$$k \parallel Y: K_{V_0} = 42 \cdot 10^{-4} \text{ kOe}^2, \quad K_{V_1}(\varphi = 45^\circ) = 541 \cdot 10^{-4} \text{ kOe}^2.$$

The calculated values agree with the measured ones (see Table II, Fig. 5 and its discussion), confirming by the same token that formula (18) in Table I describe correctly the dependence of K_V on the elastic properties of the crystal for rhombohedral antiferromagnets such as MnCO_3 . Using the value $L = 933 \text{ erg/G-cm}^3$ recalculated from [16], $H_E = 320 \text{ kOe}$, and $\rho = 3.87 \text{ g/cm}^3$ calculated from the structured data [18], from the sound velocities (22), and from the coefficients K_V (Table II), we obtain from (18) and from Table I the magnetoelastic constants for MnCO_3 :

$$\lambda_1 L^2 = (6.0 \pm 0.3) \cdot 10^6 \text{ erg/cm}^3, \quad \lambda_2 L^2 = (2.0 \pm 0.3) \cdot 10^6 \text{ erg/cm}^3.$$

7. PARAMETERS OF NUCLEAR SPIN SUBSYSTEM

The values of the parameter G , determined by reducing the experimental data (for fixed K_V from Table II) by means of formula (26), are shown in Fig. 6. As seen from the figure, the obtained values of $G(f, T)$ are well described by formula (16) and yield

$$f_{\text{nuc}0} = 638 \pm 3 \text{ MHz}$$

(which agrees with the results of measurements by the NMR method [19, 5])

TABLE II.

H	k X		k Y		k Z	
	V_3	V_2	V_{10}	V_{10}	V_{10}	V_{10}
H X	—	323 ± 15	—	—	550 ± 15	—
H Y	206 ± 15	325 ± 10	42 ± 5	—	535 ± 20	—

$$H_{\Delta 1}^2 = 0.6 \pm 0.4 \text{ kOe}^2,$$

$$H_{\Delta}^2 = \begin{cases} 1.50 \pm 0.05 \text{ kOe}^2, & T = 4.2\text{K} \\ 3.75 \pm 0.10 \text{ kOe}^2, & T = 1.65\text{K} \end{cases} \quad (30)$$

(obtained at $f_{\text{nuc}0} = 638 \text{ MHz}$), which agree with the values obtained from AFMR^[4]. The relation $H_{\Delta}^2 = bT^{-1}$ (which is connected with the dependence of the nuclear spin magnetization on the temperature), investigated in^[4], is also confirmed by our measurements (Fig. 7 shows the data for the acoustic mode (V_3, β_3, k_X), $f = 687 \text{ MHz}$, $\mathbf{H} \parallel \mathbf{X}$). From (30) we obtain $b = 6.25 \pm 0.2 \text{ kOe}^2\text{-deg}$.

8. CONCLUSION

Thus, the theoretical analysis of the behavior of a triply-connected system—electron, spin, and nuclear spin and acoustic oscillations—in rhombohedral anti-ferromagnets with easy-plane anisotropy not only describes qualitatively all the peculiarities of the peculiar magnetoacoustic resonance in MnCO_3 , which was observed by us experimentally (dependence on a magnetic field, frequency, temperature, and position of the vector \mathbf{L} in the basal plane), but is also in good qualitative agreement with the magnetic and elastic constant of MnCO_3 .

Figure 8 shows the experimental data on the variation of the speed of sound in MnCO_3 with changing magnetic field, and the theoretical plots of (26) with the values of the parameters indicated above.

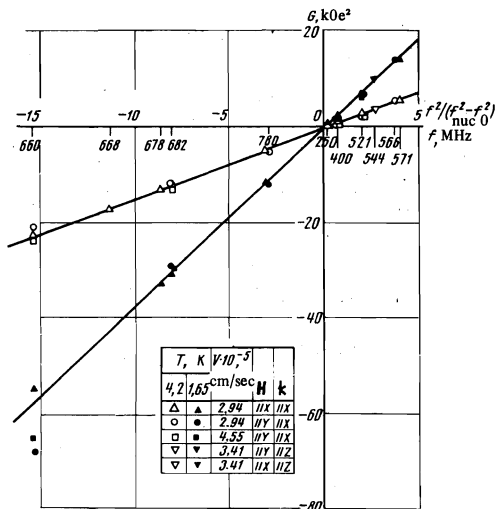


FIG. 6. Frequency of the value of G (obtained from the reduction of the experimental data by formula (26)). The theoretical lines are plots of formula (16).

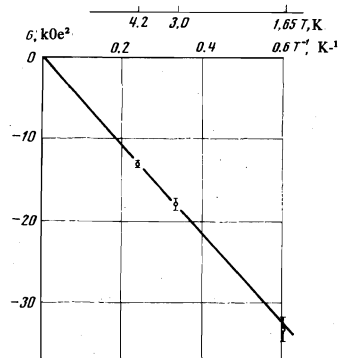


FIG. 7. Dependence of G on the temperature.

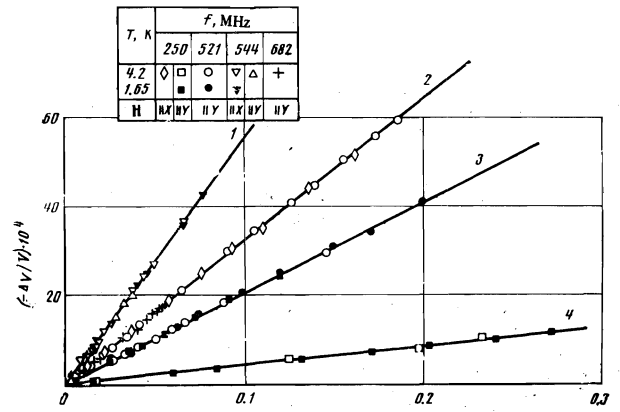


FIG. 8. Dependence of the sound velocities of different transverse acoustic modes in MnCO_3 on the quantity

$$\frac{1}{h^2 - G} \left[1 - \frac{A_2^2}{(h^2 + A_3)^2 + A_2^2} \right]$$

with the experimental values of G (see Fig. 6), A_3 and A_2 (see (28a) and (28b)). The theoretical straight lines were drawn in accordance with formula (26) with the values of K_V from Table II: 1— $k \parallel Z$, $V = 3.41$, 2— $k \parallel X$, $V = 2.94$, 3— $k \parallel X$, $V = 4.55$, 4— $k \parallel Y$, $V = 4.14$ (the velocity V is given in units of 10^5 cm/sec).

An interesting result, due to the multiply-connected nature of the oscillations, is the vanishing of the interaction between the acoustic and spin waves as $f \rightarrow f_{\text{nuc}0}$. This follows from (13) and is confirmed by our experiments.

The author is deeply grateful to Academician P. L. Kapitza for interest in the work and for the opportunity of performing it at the Institute of Physics Problems of the USSR Academy of Sciences. The author is sincerely grateful to Academician A. S. Borovik-Romanov for constant interest and guidance in the work, and is also grateful to Yu. F. Orekhov, S. M. Cheremisin, I. Ya. Krasnopolin for useful advice on problems concerning the experiment, and to B. V. Petukhov, V. G. Kamenskii for a discussion of the theoretical results, and to N. M. Kreines and V. A. Tulin for valuable discussions.

¹The author is grateful to Yu. N. Ikornikova and V.M. Egorov of the Crystallography Institute of the Academy of Sciences and to S.V. Petrov of the Semiconductor Physics Institute for useful advice on the single-crystal growth and for supplying the apparatus.

²The author is grateful to G. S. Belikova for kindly supplying the PBP crystal, and to I. M. Silverstrova and Yu. V. Pisarevskii of the Crystallography Institute of the Academy of Sciences for data on the acoustic properties of the PBP.

³ β_2 and β_3 were interchanged in^[8] in error.

⁴The author is grateful to G. G. Akalaev for help with the computer reduction of the results.

¹A. S. Borovik-Romanov, Zh. Eksp. Teor. Fiz. **36**, 766 (1959) [Sov. Phys.-JETP **9**, 539 (1960)].

²E. A. Turov, Zh. Eksp. Teor. Fiz. **36**, 1254 (1959) [Sov. Phys.-JETP **9**, 890 (1960)].

³A. S. Borovik-Romanov and E. G. Rudashevskii, Zh. Eksp. Teor. Fiz. **47**, 2095 (1964) [Sov. Phys.-JETP **20**, 1407 (1965)].

⁴A. S. Borovik-Romanov, N. M. Kreines, and L. A. Prozorova, Zh. Eksp. Teor. Fiz. **45**, 64 (1963) [Sov. Phys.-JETP **18**, 46 (1964)].

⁵A. S. Borovik-Romanov and V. A. Tulin, ZhETF Pis. Red. **1**, No. 5, 18 (1965) [JETP Lett. **1**, 134 (1965)].

⁶E. A. Turov and V. G. Kuleev, Zh. Eksp. Teor. Fiz. **49**, 248 (1965) [Sov. Phys.-JETP **22**, 176 (1966)].

- ⁷V. G. Bar'yakhtar, M. A. Savchenko, V. V. Gann, and P. V. Ryabko, *Zh. Eksp. Teor. Fiz.* **47**, 1989 (1964) [*Sov. Phys.-JETP* **20**, 1335 (1965)].
- ⁸V. R. Gakel', *ZhETF Pis. Red.* **17**, 75 (1973) [*JETP Lett.* **17**, 51 (1973)].
- ⁹E. A. Turov and M. P. Petrov, *Yadernyy magnitnyy rezonans v ferro- and antiferromagnetikakh* (Nuclear Magnetic Resonance in Ferro- and Antiferromagnets), Nauka, 1969.
- ¹⁰E. A. Turov and V. G. Shavrov, *Fiz. Tverd. Tela* **7**, 217 (1965) [*Sov. Phys.-Solid State* **7**, 166 (1965)].
- ¹¹C. Kittel, *Introduction to Solid State Physics*, Wiley, 1959.
- ¹²R. Z. Levitin, A. S. Pakhomov, and V. A. Shchurov, *Zh. Eksp. Teor. Fiz.* **56**, 1242 (1969) [*Sov. Phys.-JETP* **29**, 669 (1969)].
- ¹³A. S. Borovik-Romanov, *Magnetic Symmetry of Anti-ferromagnets*, Czechoslovak Summer School, 1965.
- ¹⁴*Physical Acoustics*, W. Mason, ed., Vol. 3B, Academic, 1966.
- ¹⁵L. A. Prozorova and A. S. Borovik-Romanov, *Zh. Eksp. Teor. Fiz.* **55**, 1727 (1968) [*Sov. Phys.-JETP* **28**, 910 (1969)].
- ¹⁶*Antiferromagnetizm i ferrity* (Antiferromagnetism and Ferrites), ed. by Ya. G. Dorfman, AN SSSR (1962).
- ¹⁷Dandekar, *J. App. Phys.*, **39**, 3695, 1968.
- ¹⁸B. F. Ormont, *Struktury neorganicheskikh veshchestv* (Structures of Inorganic Substances), Gostekhizdat (1950).
- ¹⁹D. Shaltiel, *Phys. Rev.* **142**, 300, 1966.

Translated by J. G. Adashko

197